Parametric-Gain Approach to the Analysis of DPSK Dispersion-Managed Systems

Alberto Bononi, Paolo Serena, Alessandra Orlandini, and Nicola Rossi

***Abstract*— We review a recently proposed method for bit error rate (BER) evaluation of differential phase shift keying (DPSK) long haul dispersion-managed (DM) optical systems, based on a parametric gain modeling of the nonlinear interaction between signal and amplified spontaneous emission noise along the DM transmission line. Such an interaction is responsible of nonlinear phase noise, which is the main nonlinear impairment in DPSK long-haul transmission. We review the fundamentals of the novel DPSK BER evaluation method, which extends Forestieri's method for on-off keying modulation to the DPSK case. The method avoids calculation of the nonlinear phase statistics, and accounts for intersymbol interference due to nonlinear waveform distortion, and both optical and electrical filtering. The method is critically based on the assumption of Gaussian statistics of the received optical field. In this paper, we provide further evidence of the appropriateness of the Gaussian assumption, by showing multicanonical simulations of the probability density function (PDF) of both the received optical field and of the photodetected decision variable, with a comparison to the theoretical PDF.**

I. Introduction

Optical differential phase shift keying (DPSK) offers a promising alternative to improve the performance of long-haul transmission systems [1], [2]. Compared with conventional on-off keying (OOK) format, DPSK detected with an optical delay demodulator and balanced receiver has the major benefit of a lower required optical signal-to-noise ratio (OSNR), which leads to increased system margin and extended transmission distance, or equivalently to reduced transmitted power and thus increased tolerance to fiber nonlinearities.

However, unlike OOK, the benefits of DPSK may be severely limited by nonlinear phase noise [3], i.e., the amplitude-to-phase-noise conversion due to the nonlinear interaction of signal and amplified spontaneous emission (ASE) noise during propagation. Such an interaction manifests itself also as a parametric gain (PG) of the received ASE noise. PG changes the statistics and the autocorrelation of the ASE noise process. Moreover, in presence of PG and return-to-zero (RZ) pulses whose intensity is not constant, the ASE is a non-stationary process.

Attempts have been made to theoretically study the statistics of the nonlinear phase noise in order to assess the bit error rate (BER) of DPSK receivers based on ideal phase discriminators, but an exact expression of these statistics was found only at zero group-velocity dispersion (GVD) [4], while an approximate expression including GVD based on a phenomenological argument was presented in [5].

In this paper, we review a recent alternative approach to BER evaluation, which does not need the phase noise statistics [6]. Assuming the received optical field has Gaussian statistics, and that the receiver is based on a Mach-Zehnder (MZ) balanced delay demodulator, the system BER is evaluated through a Karhunen-Loéve method for square-law detectors, which leads to a generalized chi-square distribution of the sampled current in the electrical domain, much like what done in [7], [8]. The main novelty of our work [6] is in the extension of the method to the case of non-white ASE noise before demodulation, providing a BER that accounts not only for the inter-symbol interference due to propagation, and optical and electrical post-detection filtering, but also for noise PG.

The computation of the PG statistics is a delicate matter. In conventional non-return to zero (NRZ) OOK systems, the standard method assumes a continuous wave (CW) signal (corresponding to a single mark) and studies the propagation of ASE plus such a CW. The method could clearly be applied also to NRZ-DPSK. But for return-to-zero (RZ) supporting pulses, which are the standard choice for DPSK signals, the power periodically varies in time, and so do the statistics of the PG. Although the ASE is clearly not a stationary process, in [6] we proposed, for BER evaluation, to keep using an *equivalent stationary* PG ASE process obtained from a CW signal, whose power level is a suitable filtering the time-varying intensity at the sampling time. The CW-equivalent ASE idea was tested in [6] against the correct cyclostationary ASE statistics (which can be obtained with a very

The authors are with the Dipartimento di Ingegneria dell'Informazione, Università degli Studi di Parma, Parco Area Scienze 181/A, 43100 Parma, Italy. Email: bononi@tlc.unipr.it.

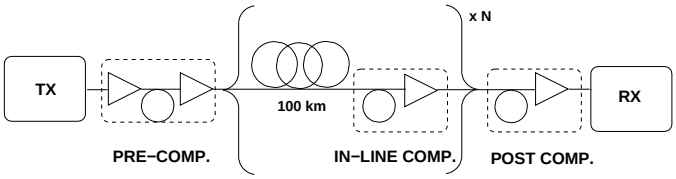

Fig. 1. Set-up of the single-channel dispersion-managed DPSK system.

computationally-expensive method [9]), with very good agreement.

The paper is organized as follows. Section II describes the DPSK long-haul DM system under study. In Section III the Gaussian assumption for the received ASE noise is discussed. Section IV derives the ASE statistics and explains the *equivalent stationary* PG ASE process. In Section V we numerically verify the accuracy of our model for BER computation against both available experimental results and multi-canonical monte-carlo (MMC) simulations [10]. Finally we provide a performance comparison of DPSK and OOK single-channel systems.

II. DPSK LONG-HAUL DM SYSTEM

Fig. 1 shows the scheme of the single-channel DPSK multi-span DM system that will be studied in the following sections. There are N identical spans, each composed of a 100 km long transmission fiber followed by a dispersion compensating fiber (in-line compensation). The in-line residual dispersion is zero (full span compensation), unless otherwise specified. Pre- and post-compensating fibers, placed before and after the transmission line, may be inserted to improve the BER. The receiver consists of a Gaussian shaped optical filter, followed by a MZ demodulator with balanced photodetection. The difference between the received currents from the two photodiodes is filtered by a Bessel 5-th order filter of bandwidth $B_e = 0.65$ time the bit rate, and then sampled.

III. RECEIVED ASE STATISTICS

The ASE noise and the transmitted signal interact during propagation through a four-wave mixing process that colors the PSD of the initially white ASE noise components, both in-phase and in-quadrature with the signal [11]. It is known that signal and ASE noise have maximum nonlinear interaction strength at zero GVD, yielding ASE statistics that strongly depart from Gaussian [4]. We already showed in [6] that the presence of a non-zero transmission fiber GVD helps reshaping the statistics of the optical field (in-phase and quadrature componnets) *before* the optical filter at the receiver, so that they are quite close to Gaussian. We want to show here that also the filtering action of the receiver optical filter helps make the statistics of the filtered optical field resemble a Gaussian bivariate density. Fig. 2(top) shows an MMC simulation of the joint probability density function (PDF) of the in-phase and quadrature components of an initially unmodulated (CW) optical field before the receiver optical filter, in the case of zero transmission fiber GVD and no DM, at a nonlinear phase rotation $\Phi_{NL} = 0.2\pi$(rad) and at a linear optical OSNR=10.8 dB/0.1nm (the one that can be read off an optical spectum analyzer, when reading the ASE power level away from the signal, where no PG exists). The PDF was obtained with 6 MMC cycles with $3 \cdot 10^6$ samples each. One can note the well known shell-like shape of the joint PDF at zero GVD [4]. Fig. 2(bottom) shows the contour plot of the PDF surface of the top figure, down to 10^{-12}.

Fig 3 shows instead the PDF contours of the same optical field, but *after* an optical filter of bandwidth of 30, 20 and 10 GHz, respectively. We clearly appreciate the tendency of the contour levels to elliptical shapes for tighter optical filtering, even in this extreme case of zero GVD. Hence we can conclude that the joint action of tight optical filtering and transmission fiber GVD both contribute to making the received optical field after optical filtering resemble a Gaussian process.

IV. MODEL FOR ASE PROPAGATION

In this section we calculate the ASE noise statistics starting from the nonlinear Schroedinger equation NLSE of a single-channel periodic dispersion-managed system. The electric field $A(z,t)$, where z is the distance and t the time normalized to the supporting pulse duration $d \cdot T$, being d the duty-cycle, propagates in its retarded time frame as:

$$\frac{\partial A}{\partial z} = j\frac{1}{2L_d(z)}\frac{\partial^2 A}{\partial t^2} - j\frac{1}{L_{NL}(z)}|A|^2 A + \frac{g(z)}{2}A \quad (1)$$

where $A(z,t)$ is normalized to the square root of the transmitted peak power P_{peak}, $L_{NL}(z) = \frac{1}{\gamma(z)P_{peak}}$ is the local nonlinear length; $L_d(z) = (d \cdot T)^2/\beta_2(z)$ is the local dispersion length referred to the supporting pulse duration; $g(z) = -\frac{1}{L_A(z)} + \Sigma_k G_k \delta(z - kL)$ is the net logarithmic gain/attenuation per unit length, where $L_A(z) = \frac{1}{\alpha(z)}$ is the fiber attenuation length, and e^{G_k} is the power gain of the k-th lumped amplifier of the link placed at $z = kL$. $\delta(.)$ indicates the Dirac delta function. $L_d(z)$, $L_{NL}(z)$, $L_A(z)$ and $g(z)$ are z-periodic functions with period equal to the span length L.

We now normalize $A(z,t)$ to the net fiber gain/attenuation up to z, i.e. $A(z,t) =$

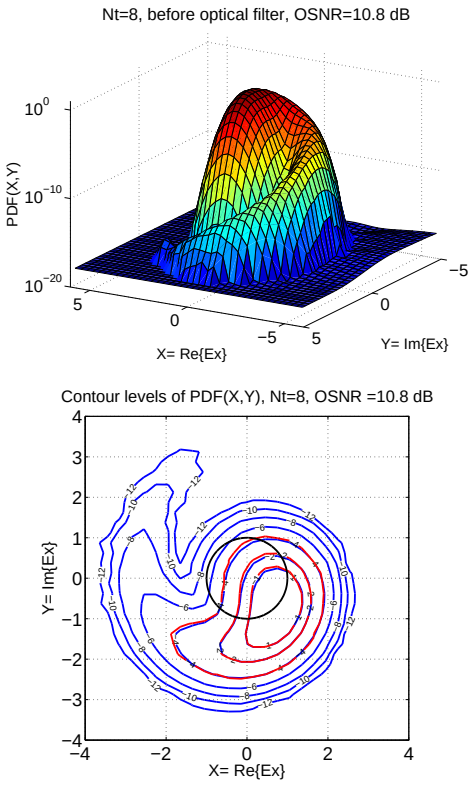

Fig. 2. (top) MMC simulated joint PDF of in-phase and quadrature components of optical field (CW+ASE) before receiver optical filter. (bottom) Contour levels of joint PDF. Data: Zero GVD, $\Phi_{NL} = 0.2\pi$(rad), linear OSNR=10.8 dB/0.1nm. MMC time samples $18 \cdot 10^6$.

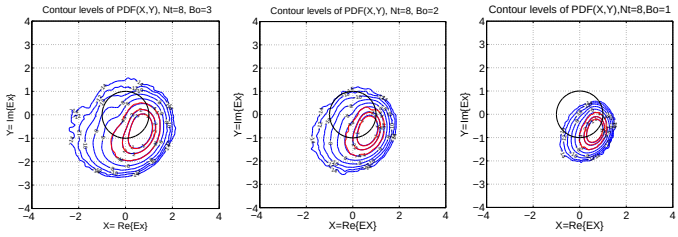

Fig. 3. Contours of MMC simulated joint PDF of in-phase and quadrature components of optical field (CW+ASE) after receiver optical filter of bandwidth (left) 30GHz, (center) 20 GHz, (right) 10 GHz. Data as in Fig. 2. Lowest contour level: 10^{-14}.

$U(z,t)e^{\frac{1}{2}\int_0^z g(x)dx} = U(z,t)\sqrt{f(z)}$, being $f(z) = \exp\left(\int_0^z g(x)dx\right)$. Thus, (1) becomes:

$$\frac{\partial U}{\partial z} = j\frac{1}{2L_d(z)}\frac{\partial^2 U}{\partial t^2} - j\frac{f(z)}{L_{NL}(z)}|U|^2 U + W_A(z,t) \quad (2)$$

where we have also included a zero-mean Gaussian noise term $W_A(z,t)$ with autocorrelation $R(z_1,z_2,t_1,t_2) = E\{W_A(z_1,t_1)W_A^*(z_2,t_2)\}$ at times t_1, t_2 and coordinates z_1, z_2 equal to:

$$R = \delta(t_1 - t_2)\,\delta(z_1 - z_2)\sum_k N_{0k}\delta(z_1 - kL)$$

where N_{0k} is the white one-sided PSD of each ASE polarization introduced by the k-th amplifier, the asterisk denotes complex-conjugate, and $E\{.\}$ indicates statistical averaging.

If the transmitted field is a CW, in absence of noise the solution of (2) is $U(z) = e^{-j\Phi_{NL}(z)}$, where $\Phi_{NL}(z) = \int_0^z f(x)\frac{1}{L_{NL}(x)}dx$ is the nonlinear phase cumulated by the CW. By adding the noise contribution, we search for a perturbed solution of (2) of the kind [11]:

$$U(z,t) = (1 + u(z,t))\,e^{-j\Phi_{NL}(z)} \quad (3)$$

where $u(z,t)$ accounts for the noise. By inserting (3) into (2), and by assuming $|u|^2 \ll 1$, so that higher-order powers of $u(z,t)$ can be dropped [9], [11], we obtain the linearized NLSE for the perturbation:

$$\frac{\partial u}{\partial z} = j\frac{1}{2L_d(z)}\frac{\partial^2 u}{\partial t^2} - j\frac{f(z)}{L_{NL}(z)}(u + u^*) + W_A \quad (4)$$

where the phase rotation Φ_{NL} in (3) has not changed the statistics of W_A. By indicating the Fourier transforms of $u(z,t)$ and $W_A(z,t)$, respectively with $\tilde{u}(z,\omega)$ and $\widetilde{W}_A(z,\omega)$, where ω is the angular frequency normalized to R/d, (4) in the frequency domain rewrites as:

$$\begin{aligned}\frac{\partial \tilde{u}}{\partial z} &= -j\frac{\omega^2}{2L_d(z)}\tilde{u}(z,\omega) \\ &\quad -j\frac{f(z)}{L_{NL}(z)}\left[\tilde{u}(z,\omega) + \tilde{u}^*(z,-\omega)\right] + \widetilde{W}_A(z,\omega) \quad (5)\end{aligned}$$

Thanks to its z-periodic behavior, the local dispersion length can be written as $\frac{1}{L_d(z)} = \frac{1}{L_D} + \frac{1}{L_\Delta(z)}$, where $\frac{1}{L_D} = \frac{1}{L}\int_0^L \frac{1}{L_d(x)}dx$ is the inverse span-averaged dispersion length, while $1/L_\Delta$ accounts for the local deviation from such an average. Inside each span, we recognize two different dynamics along z due to the fiber dispersion, a *slow* dynamic due to L_D and a *fast* dynamic due to L_Δ. We next move into a reference system that follows the fast dynamic by making the change of variable:

$$\tilde{u}(z,\omega) = \tilde{a}(z,\omega)e^{-j\frac{\Theta_\Delta(z,\omega)}{2}} \quad (6)$$

being $\Theta_\Delta = \omega^2\int_0^z \frac{1}{L_\Delta(x)}dx$. Substituting (6) in (5) yields:

$$\begin{aligned}\frac{\partial \tilde{a}}{\partial z} &= -j\frac{\omega^2}{2L_D}\tilde{a}(z,\omega) - j\frac{f(z)}{L_{NL}(z)} \\ &\quad \cdot\left[\tilde{a}(z,\omega) + \tilde{a}^*(z,-\omega)e^{j\Theta_\Delta}\right] + \widetilde{W}_A(z,\omega) \quad (7)\end{aligned}$$

where again the phase rotation in (6) does not change the Gaussian statistics of the noise $\widetilde{W}_A$. For a finite received nonlinear phase, when the number of spans $N \to \infty$, the

infinitesimal nonlinear phase rotation per span turns out to drive the evolution of $a(z,\omega)$ as a slowly-varying z-function span by span. Thus, using the method of averaging, we substitute the rapidly varying terms in (7) with their span-averaged values:

$$\left\langle \frac{f(z)e^{j\Theta_\Delta(z,\omega)}}{L_{NL}(z)} \right\rangle = \frac{1}{L}\int_0^L \frac{f(x)e^{j\Theta_\Delta(x,\omega)}}{L_{NL}(x)}dx \triangleq \mathcal{R}(\omega)\,. \tag{8}$$

Introducing the *kernel* of the transmission link $r(\omega) \triangleq \mathcal{R}(\omega)/\mathcal{R}(0)$ [14], (7) rewrites as:

$$\begin{aligned}\frac{\partial \tilde{a}}{\partial z} &= -j\frac{\omega^2}{2L_D}\tilde{a}(z,\omega) - j\mathcal{R}(0) \\ &\quad \cdot [\tilde{a}(z,\omega) + \tilde{a}^*(z,-\omega)r(\omega)] + \widetilde{W}(z,\omega)\end{aligned} \tag{9}$$

where, thanks to the method of averaging, we substituted the white ASE $\widetilde{W}_A$ with a Langevin Gaussian noise process $\widetilde{W}$ with PSD at coordinates (z_1, z_2) equal to $E\left\{\widetilde{W}(z_1,\omega)\widetilde{W}^*(z_2,\omega)\right\} = 2\sigma^2\delta(z_1 - z_2)$, being $2\sigma^2$ the one-sided ASE PSD per unit length. For an N-span link it is $2\sigma^2 NL = \sum_{k=1}^{N} N_{0k}$. In terrestrial systems having long spans ($L \gg L_A$), we find

$$r(\omega) \cong \frac{1}{1 + jS\omega^2} \tag{10}$$

where we call $S \triangleq -\frac{L_A}{L_\Delta}$ the *map strength* of the terrestrial DM system [6], and we associate to S the sign of the transmission fiber dispersion D_{tx}. It is also $\mathcal{R}(0) = \frac{L_A}{L}\cdot\frac{1}{L_{NL}}$, which corresponds to the inverse span-averaged nonlinear length. Note that all parameters in the system lengths L_A, L_{NL}, L_Δ refer to the transmission fiber.

The stationary Gaussian noise $\tilde{a}(z,\omega)$ has in-phase and quadrature components whose PSD matrix (normalized to the case in absence of PG) is defined as:

$$\mathbf{G}(z,\omega) \triangleq \begin{bmatrix} G_{pp} & G_{pq} \\ G_{qp} & G_{qq} \end{bmatrix} \triangleq \frac{\mathbf{E}\left\{\tilde{\mathbf{a}}(\mathbf{z},\omega)\tilde{\mathbf{a}}^\dagger(\mathbf{z},\omega)\right\}}{\sigma^2 z}$$

where $\sigma^2 z$ is the variance per component in absence of PG. It is proven in [6] that

$$\mathbf{G}(z,\omega) = k_0\mathbf{I} - k_1\begin{bmatrix} -r_i & r_r \\ r_r & r_i \end{bmatrix} - k_2\begin{bmatrix} r_r & r_i \\ r_i & -r_r \end{bmatrix} \tag{11}$$

where

$$\begin{cases} k_0 = & 1 + 4\Phi_{NL}^2(z)\frac{|r|^2}{(2kz)^2}\left(\frac{\sinh 2kz}{2kz} - 1\right) \\ k_1 = & 2\Phi_{NL}(z)\frac{\cosh 2kz - 1}{(2kz)^2} \\ k_2 = & 4\Phi_{NL}(z)\left(\frac{z}{L_D}\frac{\omega^2}{2} + \Phi_{NL}(z)\right)\frac{1}{(2kz)^2}\left(\frac{\sinh 2kz}{2kz} - 1\right) \end{cases}$$

being $r(\omega) = r_r + jr_i$ the kernel, $\Phi_{NL}(z) = z\mathcal{R}(0)$ the cumulated nonlinear phase by the CW, and

$$kz = \sqrt{\Phi_{NL}^2(z)\mid r(\omega)\mid^2 - \left(\frac{\omega^2}{2}\frac{z}{L_D} + \Phi_{NL}(z)\right)^2}\,.$$

If the link is followed by a linear device, e.g. a dispersion compensating fiber and/or an optical filter, with tranfer matrix $H(\omega)$, the output PSD matrix becomes $HGH^\dagger$. In the limit $\omega \longrightarrow 0$ we have $G_{pp} \longrightarrow 1$ and $G_{qq} \longrightarrow 1 + \frac{4}{3}\Phi_{NL}^2$, hence at large Φ_{NL} the quadrature component is dominant and manifests itself as nonlinear phase noise.

It is easy to verify that (9) is a linearization of the DM-NLSE of Ablowitz *et al.* [14]. We verified that the DM-NLSE yields very accurate PSDs when the nonlinear phase rotation per span is roughly below 0.02 rad, and qualitatively reasonable results up to nonlinear phase rotations per span of 0.1 rad.

Closer examination of (11) reveals that, in the long-span terrestrial map case whose kernel $r(\omega)$ is given in (10), the ASE PSD solely depends on the three following dimensionless parameters: i) the strength S; ii) the normalized average in-line dispersion $\frac{z}{L_D}$; iii) the peak nonlinear phase $\Phi_{NL}(z) = \frac{z}{L_{NL}}\frac{L_A}{L}$. Such three parameters provide general scaling rules both for the noise parametric gain analysis and for the general design of DM terrestrial systems.

A. Effects of pulse shape on ASE

Since the proposed ASE model is based on a CW assumption for the signal, it does not take into account the influence of signal modulation and pulse shape.

In [6] we found that the CW-equivalent model still applies by using as the CW reference power a proper effective value $P_{eff}(t_s)$ at sampling times t_s. The intuition about the appropriate value of P_{eff} comes from equation (9), which reveals that, at a specific ω, the noise field gets energy from the CW only within a proper frequency bandwidth. Such a bandwidth, which is essentially set by the bandwidth of the kernel $r(\omega)$, corresponds to a finite memory window in the time domain. Hence we expect that the effective power $P_{eff}(t)$ to be a filtered version of the transmitted power $P(t)$ over such a time window. For instance, in the limit of a very narrow time window, $P_{eff}(t)$ should coincide with the local power at time t (thus $P_{eff}(t_s) = P_{peak}$), while for a very large memory time window the noise interacts with the average power on such a window (thus $P_{eff}(t_s) = \overline{P}$). For the terrestrial kernel (10) we empirically found that a proper windowing filter for a fully-compensated system is:

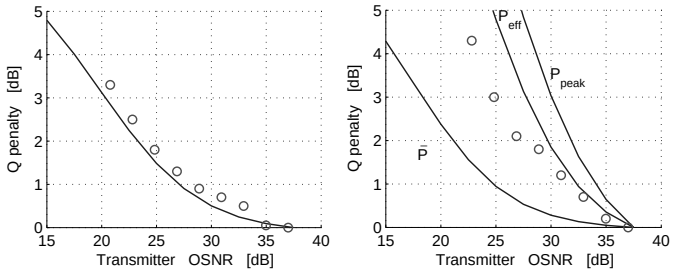

Fig. 4. Q-penalty versus transmitter OSNR for NRZ- (left) and RZ-DPSK (right) for the experimental system tested by Kim et al. in [12] with a launched power of 7 dBm and $d = 0.33$.

$$H(\omega) = \frac{1}{1 + \left(\frac{S}{4}\omega^2\right)^2} \tag{12}$$

so that $P_{eff}(t) = P(t) \otimes h(t)$, being $h(t)$ the inverse Fourier transform of $H(\omega)$, while $\otimes$ denotes convolution. Hence, the quasi-stationary ASE noise PSD at time t_s can still be evaluated from (11), in which we use $P_{eff}(t_s)$ in place of P_{peak} in the evaluation of Φ_{NL}.

V. Results and Discussion

In this section we prove the accuracy of our model for BER evaluation in presence of PG by checking it against experimental and numerical results. The procedure to evaluate BER once the statistics of the Gaussian received ASE are known is discussed in detail in [6]. Here we provide some numerical results.

We first reproduced the experimental results of Kim *et al.* in [12] for a 6×100 km non-zero dispersion shifted single-channel link working at $R = 10$ Gb/s and with a launched power of 7 dBm. Fig. 4 shows the Q-factor penalty measured in [12] with circles and the prediction of our model (solid line) for (left) NRZ- and (right) RZ-DPSK ($d = 0.33$). Note that in our method the Q-factor is evaluated by inverting the analytical BER. In each curve the penalty is referred to the Q factor at a transmitter OSNR=37 dB, which is the highest value used in the experiment. For the details of the system set-up see [12]. For the RZ case, we evaluated the Q penalty by using the CW-equivalent ASE model with either the average power $\overline{P}$, or the peak power P_{peak}, or the effective power P_{eff} obtained through (12). From the comparison with experimental data, the case using P_{eff} is found to reasonably fit the experimental data up to penalties of 2 dB, with some over-estimation at lower values of OSNR.

In Fig. 5(top) we checked the analytical PDF of the sampled current at the decision gate against that obtained through direct simulation with the MMC method. Results are shown for a 20×100km link, with transmission fiber GVD $D_{Tx} = 4$ ps /nm/km and positive in-line dispersion

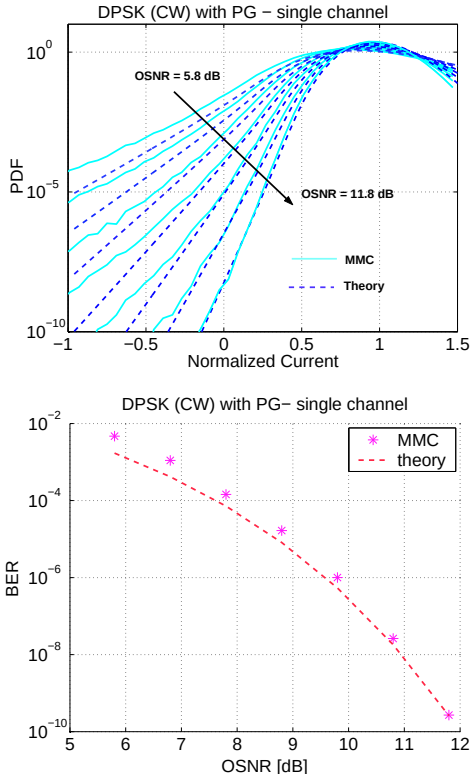

Fig. 5. (top) PDF of sampled current: MMC (solid), theory (dashed) for several values of linear OSNR (dB/0.1nm). (bottom) BER obtained from above PDFs (symbols) and from theory (dashed). Data: 20x100 km, $D_{TX} = 4$ps/nm/km , $D_{pre} = 0$, $D_{inline} = 40\, ps/nm/span$, $D_{post} = 0$, $\Phi_{NL} = 0.2\pi$(rad). R=10 Gb/s. Optical filter bandwidth 1.8R.

$D_{in} = 40$ ps/nm per span. The nonlinear phase was 0.2π(rad), and a single 10Gb/s NRZ-DPSK channel was transmitted with a pattern 1,1,1,1.... actually corresponding to a CW signal. The OSNR (dB/0.1nm) was varied from 5.8 dB, where the nonlinear effect of PG is strong, to 12.8 dB. No pre and post-compensation was used here. An improving match between MMC and theoretical PDFs is observed for increasing OSNR. Fig. 5(bottom) shows the BER obtained by integrating the tail of the PDFs below the zero threshold. We notice that the theory based on the Gaussian assumption for the received optical field gives an excellent prediction of the true BER, with half of a dB of discrepacy at the lowest OSNR, i.e. at BER values worse than 10^{-4}.

A. Comparison with OOK

Finally, we compared the Q-factor of DPSK format with the one of an OOK modulation with NRZ pulses. For OOK we evaluated the BER as in [13]. A peculiar difference is that for OOK the PG effects appear only at large nonlinear phases [13]. Hence the ASE PSD for OOK at nonlinear phase values beyond the accuracy of (11)

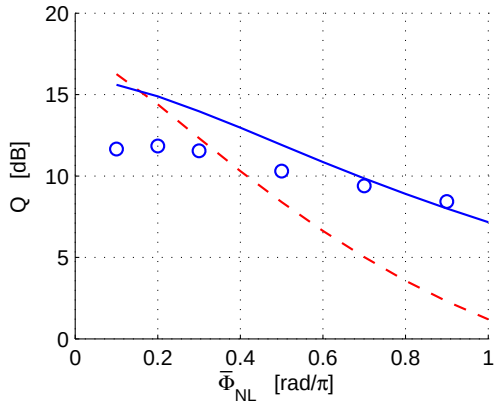

Fig. 6. Q-factor vs. average $\overline{\Phi}_{NL}$ for NRZ-DPSK (solid), RZ-DPSK at 50% duty-cycle (dashed) and NRZ-OOK (circles). 20×100 km fully compensated system at $R = 10$ Gb/s ($S = 0.02$ for $D_{tx} = 8$ ps/nm/km), OSNR=11 dB/0.1 nm.Optical filter bandwidth 1.8 R.

were estimated through off-line Monte Carlo simulations, as detailed in [13]. For DPSK, instead, we used the analytical ASE PSD (11) since the performance rapidly deteriorates already at small nonlinear phases.

The optical link was again a 20x100 km, with transmission fiber GVD $D_{TX} = 8$ps/nm/km, fully compensated at each span, with optimized pre and post-compensation for each format at each nonlinear phase value. The linear OSNR at the receiver was 11dB/0.1 nm. Fig. 6 depicts the measured Q-factor vs. the average nonlinear phase $\overline{\Phi}_{NL}$, for NRZ-DPSK (solid), 50% RZ-DPSK (dashed) and NRZ-OOK (circles). From the figure we note the well known 3 dB difference between DPSK and OOK at small $\overline{\Phi}_{NL}$, while for increasing $\overline{\Phi}_{NL}$ we observe different distortions on the modulation formats, mainly due to PG. We note that RZ-DPSK is strongly affected by PG since in this case P_{eff} is close to P_{peak}, twice the value than in NRZ-DPSK. Meanwhile, we observe that OOK for increasing $\overline{\Phi}_{NL}$ recovers the previously mentioned 3 dB gap, and it overcomes DPSK at large $\overline{\Phi}_{NL}$. The reason can be found in the greater PG-induced increase of the noise quadrature component with respect to the in-phase one. Such an inflation has a strong impact in terms of nonlinear phase noise on the performance of DPSK.

VI. Conclusions

We reviewed the DPSK BER evaluation method in presence of PG that we recently proposed in [6]. The critical assumption of Gaussian statitics of the received optical field at the optical receiver was further supported by novel comparisons with accurate simulations using the multi-canonical monte carlo method.

Acknowledgment

This work was supported by a research grant of Alcatel R&I, France. The authors wish to thank G. Charlet, J.-C. Antona and S. Bigo for invaluable feedback on the work, and A. Vannucci for advice on the MMC simulations.

References

[1] A. H. Gnauck and P. J. Winzer, "Optical Phase-Shift-Keyed Transmission", *J. Lightwave Technol*., vol. 23, pp. 115-130, Jan. 2005.

[2] G. Charlet, E. Corbel, J. Lazaro, A. Klekamp, R. Dischler, P. Tran, W. Idler, H. Mardoyan, A. Konczykowska, F. Jorge and S. Bigo, "WDM transmission at 6-Tbit/s capacity over transatlantic distance, using 42.7-Gb/s differential phase-shift keying without pulse carver," *J. Lightwave Technol*., vol. 23, pp. 104-107, Jan. 2005.

[3] J.-P. Gordon and L. F. Mollenauer, "Phase noise in photonic communications systems using linear amplifiers," *Opt. Lett*., vol. 15, no. 23, pp. 1351-1353 , Dec. 1990.

[4] K.-P. Ho, "Probability density of nonlinear phase noise," *J. Opt. Soc. Am. B*, vol. 20, pp. 1875-1879, Sept. 2003. For a more comprehensive documentation, see also K.-P. Ho, "Statistical properties of nonlinear phase noise," at http://arxiv.org/abs/physics/0303090, last updated Sept. 2005.

[5] Y. Yadin, M. Shtaif and M. Orenstein, "Nonlinear phase noise in phase modulated WDM fiber-optic communications," *IEEE Photon. Technol. Lett.*, vol. 16, pp. 1307-1309, May 2004.

[6] P. Serena, A. Orlandini, and A. Bononi, "Parametric-gain approach to the analysis of single-channel DPSK/DQPSK systems with nonlinear phase noise," *J. Lightwave Technol.*, vol. 24, pp. 2026-2037, May 2006.

[7] E. Forestieri, "Evaluating the error probability in lightwave systems with chromatic dispersion, arbitrary pulse shape and post-detection filtering," *J. Lightwave Technol.*, vol. 18, pp. 1493-1503, Nov. 2000.

[8] J. Wang and J. M. Kahn, "Impact of chromatic and polarization-mode dispersions on DPSK systems using interferometric demodulation and direct detection," *J. Lightwave Technol.*, vol. 22, pp. 362-371, Feb. 2004.

[9] R. Holzlöhner, V.S. Grigoryan, C.R. Menyuk, and W. L. Kath, "Accurate calculation of eye diagrams and bit error rates in optical transmission systems using linearization," *J. Lightwave Technol*., vol. 20, pp. 389-400, March 2002.

[10] R. Holzlöhner, and C.R. Menyuk, "Use of multicanonical monte carlo simulations to obtain accurate bit error rates in optical communications systems," *Opt. Lett.*, vol. 28, pp. 1894-1896, Oct. 2003.

[11] A. Carena, V. Curri, R. Gaudino, P. Poggiolini and S. Benedetto, "New analytical results on fiber parametric gain and its effects on ASE noise," *IEEE Photon. Technol. Lett.*, vol. 9, pp. 535-537, Apr. 1997.

[12] H. Kim and A. H. Gnauck, "Experimental investigation of the performance limitation of DPSK systems due to nonlinear phase noise," *IEEE Photon. Technol. Lett*., vol. 15, pp. 320-322, Feb. 2003.

[13] P. Serena, A. Bononi, J. C. Antona and S. Bigo, "Parametric gain in the strongly nonlinear regime and its impact on 10 Gb/s NRZ systems with forward-error correction," *J. Lightwave Technol*., vol. 23, pp. 2352-2363, Aug. 2005.

[14] M. J. Ablowitz, and T. Hirooka, "Managing nonlinearity in strongly dispersion-managed optical pulse transmission," *J. Opt. Soc. Am. B*, vol. 19, pp. 425-439, March 2002.